BMC Plant Biology

RESEARCH Open Access

Assessment of suitable habitat of *Semen Armeniacae Amarum*. in China under different climatic conditions by Internal Transcribed Spacer 2 and Maxent model

Donglai Ma[1,2†], Zikang Lu[1†], Zhiqiang Xue[3], Zihan Yu[1], Xuhong Duan[1], Xian Gu[1], Yukun Yao[1*], Le Cai[1*] and Kaiyan Zheng[1,2*]

Abstract

Semen Armeniacae Amarum is a Chinese medicine. The Chinese Pharmacopoeia stipulates that the dried ripe seeds of these four plants *(Prunus armeniaca* L. var. ansu Maxim., *Prunus sibirica* L., *Prunus mandshurica* (Maxim.) Koehne, and *Prunus armeniaca* L.) can all be used as *Semen Armeniacae Amarum*. Amygdalin is widely recognized as a key quality marker for standardizing *Semen Armeniacae Amarum*. It exhibits notable antitussive and antiasthmatic effects, and is believed to relieve cough by modulating the activity of the respiratory center. Its diverse pharmacological properties position it as a potential lead compound in drug discovery and the development of novel therapeutics. Climate change has a significant impact on distribution of the aforementioned species and the accumulation of their bioactive components. In this study, the distribution site information of all four plant species was collected through field surveys and online data surveys. Using the Internal Transcribed Spacer 2 (ITS2), the attribution of bitter almonds in each species from different geographical region was identified and the amygdalin content was measured. The maximum entropy model was coupled with the stepwise regression algorithm to evaluate the potential impact of future climate on the quality of amygdalin. The results showed that the 26 samples collected from different producing areas were all identified as PS. Under various Representative Concentration Pathway (RCP2.6, RCP4.5, and RCP8.5), the projected future distribution ranges of *Prunus sibirica* L. (PS) and *Prunus armeniaca* L. (PA) are predicted to contract, whereas the range of *Prunus mandshurica* (Maxim.) Koehne (PK) is projected to expand slightly. The distribution range of *Prunus armeniaca* L. var. ansu Maxim. (PM) is expected to either expand or contract, depending on specific scenarios and timeframes. Specifically, an expansion is projected under RCP2.6 in both the 2050s and 2070s, and under RCP8.5 in the 2050s. Conversely, a contraction is

†Donglai Ma and Zikang Lu contributed equally to this work.

*Correspondence:
Yukun Yao
41399932@qq.com
Le Cai
hebcmyzb@126.com
Kaiyan Zheng
zhengkaiyan168@126.com

Full list of author information is available at the end of the article

projected under RCP4.5 in the 2050s and 2070s, and under RCP8.5 in the 2070s. From the perspective of secondary metabolism, amygdalin content exhibits a strong positive correlation with temperature and precipitation. These findings provide valuable guidance for optimizing traditional medicine supply chains and formulating targeted conservation strategies for medicinal resources.

Clinical trial number
Not applicable.

Keywords Amygdalin, ITS2, Climate changes, Quality variation, Species distribution

Introduction

Climate change is a key factor influencing plant distribution and growth [1]. The growing global population, rising energy consumption, and increasing carbon emissions are intensifying the global warming of the climate, with increasingly severe consequences anticipated in the future [2]. Under climate warming, the phytochemical composition of traditional medicinal plants is expected to undergo substantial alterations [3, 4]. Understanding how plants (especially medicinal species) respond to climate change, and forecasting their potential future distributions under varying climate scenarios, is crucial for developing targeted management and conservation strategies [5]. *Semen Armeniacae Amarum.* (SAA), derived from the dried mature seeds of *Prunus armeniaca* L. var. ansu Maxim. (PM), *Prunus sibirica* L. (PS), *Prunus mandshurica* (Maxim.) Koehne (PK), and *Prunus armeniaca* L. (PA), is widely used in clinical practice as a traditional Chinese medicine. However, SAA is currently confronted with several critical challenges. Existing processing technologies remain underdeveloped, and there is a lack of high-value, technology-driven derivative products. As a result, the overall resource utilization rate remains low, resulting in considerable material waste [6]. Although none of the four botanical sources of SAA are included in the IUCN Red List of Threatened Species, they are extensively utilized, and their distinct ecological niches and geographic distributions result in pronounced variability in SAA quality. Amygdalin, the principal active component of SAA, has been extensively studied for its pharmacological properties. As a secondary metabolite, the accumulation of amygdalin is highly sensitive to fluctuations in temperature and precipitation [7]. Therefore, investigating the influence of climatic variables on both the spatial distribution of the four SAA source species and amygdalin biosynthesis is of critical importance.

SAA has a bitter taste, slightly warm, and is mildly toxic, acting primarily on the lung and large intestine meridians [8]. It is believed to help reduce lung qi, relieve cough and asthma, and moisten the intestines to alleviate constipation. It is commonly used to treat cough, asthma, chest fullness with abundant phlegm, and intestinal dryness with constipation [9]. SAA primarily grow in China, the United States, India, Russia, Iran, Italy, and several other countries. Studies have indicated that amygdalin possesses antioxidant, antitumor, antifibrotic, anti-atherosclerotic, anti-inflammatory, immunomodulatory, and analgesic properties, with the ability to improve conditions across various systems, including the digestive, reproductive, neurodegenerative, and myocardial hypertrophy systems [10]. Other have reported that amygdalin influences cancer cell adhesion and migration [11], exhibits significant antitumor activity in both castration-sensitive and castration-resistant prostate cancer cell lines and warrants further evaluation for therapeutic purposes [12], exhibits potent, broad-spectrum antimicrobial activity against various pathogenic microorganisms [13]. Furthermore, amygdalin serves as a standard indicator for content determination of SAA in the Chinese Pharmacopoeia, underscoring its significance. Global climate change not only affects the migration and distribution of medicinal plant habitats but also induces changes in their pharmacologically active components [14]. Given the diverse origins of SAA and the varying quality among different varieties, studying the impact of climate change on the accumulation of pharmacologically active compounds becomes even more critical. There are numerous studies on the distribution simulation of medicinal plants [15–19]. Common analysis and prediction are carried out by collecting samples on a large scale but in several cases the variants or the original plant sources are uncertain. In this study we used the Internal Transcribed Spacer 2 (ITS2) technology to identify the original plant sources of the collected samples, and then combine it with the amygdalin content determined by HPLC to conduct a quality zoning analysis. Species distribution models (SDMs) are employed to assess the impact of climate change on the potential distribution of species [20]. The maximum entropy model (Maxent) is widely applied to evaluate the environmental requirements for species growth and the suitability of their distribution. Studies have shown that, Maxent offers superior predictive power and stability [21], as well as advantages such as simplicity, convenience, and minimal sample size requirements [22]. The Geographic Information System (GISs) integrates ecological factors, such as climate type, vegetation type, and soil texture, into data layers based on ecological principles and analytical methods, facilitating

accurate quantification of species' potential distribution areas through vector calculations.

Our study projected the climatic range of four SAA producing tree species and the amygdalin quality zoning of one of those species. By doing so we aimed to investigate the primary climatic factors affecting the distribution of those SAA producing species and identify their optimal climatic areas.

Materials and methods

Species occurrence data

Distribution records for the four plant species were obtained from the Chinese Virtual Herbarium (https://www.cvh.ac.cn/) and the Global Biodiversity Informati on Facility (https://www.gbif.org). Duplicate and clearly erroneous latitude and longitude records were excluded to minimize sampling bias and avoid the inclusion of identical points. The "fishing net" method was applied to filter out records with geographically redundant locations [23]. Due to the large scale of the study, data filtering methods from previous research were applied, and the samples were ultimately screened using a 16 km × 16 km geographic grid [24–25]. For multiple samples within the same grid cell, one point near the center was selected as the representative sample. As a result, 51 occurrence records of PM, 85 occurrence records of PS, 46 occurrence records of PK, and 186 occurrence records of common PA were collected (Fig. 1). Samples for amygdalin content determination were collected by Chengde Yaou Nuts & Seeds Co.,Ltd., for 26 samples from various production areas. The sampling sites covered all major production regions of SAA across China, and approximately 5 kg of material were collected from each location in September.

Species identification based on ITS2

We commissioned BGI Genomics (Shanghai) Co., Ltd. to conduct ITS2 sequencing on samples from 26 regions to identify their origins and perform a quality zoning analysis. DNA was extracted using the Ezup Column Plant Tissue Genomic DNA Extraction Kit. The upstream primer used for PCR amplification was ITS2 2F: 5'-ATGCGATACTTGGTGTGAAT-3', and the downstream primer was ITS23R: 5'-GACGCTTCTCCAGAGACTACAAT-3'. The PCR amplification system had a final volume of 25 μL, which included 2.5 μL of Taq Buffer (with MgCl2, final concentration: 10×), 1 μL of DNA template, 1 μL each of the upstream and downstream primers, 0.2 μL of Taq enzyme, 1 μL of dNTP mix, and ddH_2O to reach a final volume of 25 μL. The amplification program involved the following steps: initial denaturation at 95 °C for 5 min, followed by 10 cycles of denaturation at 94 °C for 30 s, annealing at 63 °C for 30 s, and extension at 72 °C for 30 s; then 30 cycles of denaturation at 95 °C for 30 s, annealing at 58 °C for 30 s, and extension at 72 °C for 30 s; and a final extension at 72 °C for 10 min. Phylogenetic analysis was conducted using MEGA 6.0 software, based on sequences from 26 sample batches and those retrieved from GenBank (https://www.ncbi.nlm.nih.gov/genbank/) [26]. GenBank registration login number: AJ746592.1、AJ746592.1 and AJ746592.1.

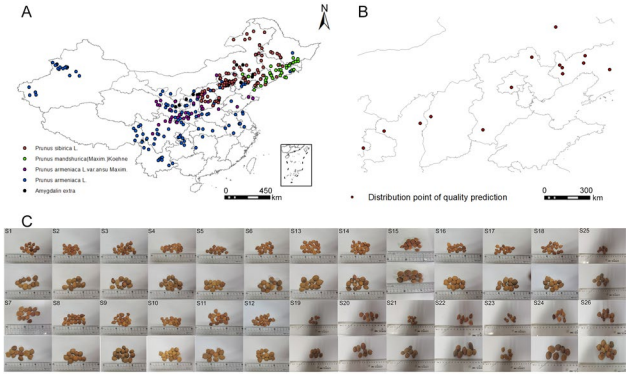

Fig. 1 Distribution records in China (**A**), contents of 14 amygdalin in *Prunus sibirica* L. (**B**), appearance of 26 batches of samples (**C**)

Chemical composition analysis

The amygdalin content in SAA was quantified according to the method outlined in the Chinese Pharmacopoeia [8]. All samples were analyzed in triplicate to ensure reproducibility. The average concentration was subsequently calculated. Reference and test sample solutions were prepared according to the content determination protocol for SAA outlined in the *Pharmacopoeia of the People's Republic of China* (2020 edition). Chromatographic column: InertSustain C18 (5 μm, 4.6 mm × 250 mm); Mobile phase: acetonitrile-0.1% phosphoric acid solution (8:92); Flow rate: 1 mL/min; Detection wavelength: 207 nm; Column temperature: 30 °C; Injection volume: 10 μL.

Environmental variables

Firstly, we selected 19 bioclimatic variables. (Table 1). Climate data for the current period (1970–2000) and two future periods, the 2050s (2041–2060) and the 2070s (2061–2080), were obtained from the global climate database (http://www.worldclim.org/). The future climate data include three greenhouse gas emission scenarios (RCP2.6, RCP4.5, and RCP8.5) from the Intergovernmental Panel on Climate Change (IPCC) Fifth Assessment Report, corresponding to low, medium, and high emission levels, respectively [27]. Due to the inability to unify the resolution of the data downloaded from the IPCC Sixth Assessment Report, we opted to use data from the IPCC Fifth Assessment Report for our study. The Community Climate System Model version 4 (CCSM4) model, which demonstrates strong simulation

Table 1 The 19 environmental variables in the maxent model

No.	Description	Abbreviation
1	Annual Mean Temperature (℃)	Bio1
2	Mean Diurnal Range (℃)	Bio2
3	Isotherm (Bio2/Bio7) (×100)	Bio3
4	Temperature Seasonality	Bio4
5	Maximum Temperature of the Warmest Month (℃)	Bio5
6	Minimum Temperature of the Coldest Month (℃)	Bio6
7	Temperature Annual Range (℃)	Bio7
8	Mean Temperature of the Wettest Quarter (℃)	Bio8
9	Mean Temperature of the Driest Quarter (℃)	Bio9
10	Mean Temperature of the Warmest Quarter (℃)	Bio10
11	Mean Temperature of the Coldest Quarter (℃)	Bio11
12	Annual Precipitation (mm)	Bio12
13	Precipitation of the Wettest Period (mm)	Bio13
14	Precipitation of the Driest Period (mm)	Bio14
15	Precipitation Seasonality of CV	Bio15
16	Precipitation of the Wettest Quarter (mm)	Bio16
17	Precipitation of the Driest Quarter (mm)	Bio17
18	Precipitation of the Warmest Quarter (mm)	Bio18
19	Precipitation of the Coldest Quarter (mm)	Bio19

capabilities in China [28], was employed for generating the future climate data. The spatial resolution of the environmental factors was set to 1 km × 1 km. Correlations among variables can violate statistical assumptions and result in predictive overfitting. To address this issue, we applied Pearson correlation analysis to screen the 19 bioclimatic variables. Among the environmental variables with high collinearity ($r > 0.8$), we retained those with a significant influence on the growth of the four focal plant species[29]. Given that the jackknife test demonstrated the relative importance of each environmental factor, we performed a Maxent model run to obtain both the contribution rates and jackknife plots. Based on both the correlation matrix and the jackknife results, we identified the variables with the greatest influence on the distribution of the four target species[30]. Subsequently, taking into account the actual growth conditions of the focal species as well as literature on the environmental responses of bitter almond source plants and closely related taxa-we retained a subset of variables for further analysis [31–33]. Thirteen bioclimatic variables were selected for PK, thirteen for common PA, fourteen for PM, and fourteen for PS for the Maxent modeling (Table 2).

Distribution modeling and model evaluation

Initially, geographic coordinate data and environmental factors for seven distinct time periods were incorporated into the Maxent software. To guarantee adequate convergence time, we set a limit of 10,000 for the maximum number of background points and restricted the maximum number of iterations to 3000. The Maxent model was fed with an ASCII code file containing information about the geographical distribution and environmental factors of the four SAA species. A random selection of 75% of the distribution data was utilized to develop the model, with the remaining 25% reserved for testing and validation purposes. We iteratively ran the Maxent model, removing variables with zero contribution at each step, and repeated this procedure ten times to derive the final set of contributing factors. Using the jackknife method, each environmental variable was detected for relative importance [34]. To further investigate influence by environmental factors species distribution suitability, the response curves of these factors were analyzed. The response curves illustrate the relationship between environmental factors and species suitability. We used the area under the curve (AUC) of receiver operating characteristics (ROC) and adjusted for use with presence-only data (transformed AUC, tAUC) in accordance with Halvorsen [35], as a measure of model performance. tAUC= (AUC-ϕ/2)/ (1-ϕ), where ϕ is the number of presence observations divided by the number of background observations. In this study, an AUC value greater than 0.9 was considered indicative of high predictive accuracy of the model [36–37]. tAUC values above 0.9 indicate 'very good' predictive performance [38]. Subsequently, the results from the Maxent model were imported into ArcGIS 10.8 software. In ArcGIS, suitable habitats were classified into four levels based on the habitat suitability values of the species distribution points, using the natural breaks classification method: unsuitable (0.0-0.2), low suitability (0.2–0.4), medium suitability (0.4–0.6), and high suitability (0.6-1) [30]. This step was performed using the mapping and classification tools in ArcGIS 10.8, ultimately generating the species' potential distribution map [39].

Quality regionalization of PS

We selected samples with amygdalin content greater than 3% in accordance with the provisions of the Chinese Pharmacopoeia 2020 edition for further analysis

Table 2 Environmental factors used for analysis after correlation screening

Species	Variable
PM	Bio1 Bio2 Bio3 Bio5 Bio6 Bio7 Bio8 Bio10 Bio12 Bio14 Bio16 Bio17 Bio18 Bio19
PA	Bio1 Bio2 Bio3 Bio4 Bio5 Bio 7Bio8 Bio10 Bio12 Bio15 Bio16 Bio17 Bio19
PS	Bio1 Bio2 Bio3 Bio4 Bio5 Bio6 Bio7 Bio8 Bio10 Bio12 Bio15 Bio16 Bio17 Bio18
PK	Bio2 Bio3 Bio4 Bio5 Bio7 Bio8 Bio10 Bio12 Bio14 Bio 15 Bio16 Bio17 Bio19

[40]. Stepwise regression analysis was conducted on the environmental factors and amygdalin content of the PS samples using SPSS 27.0 [41]. The content of amygdalin is regarded as the dependent variable, while the environmental factors are considered as the independent variables. The method selected is stepwise, with an p-value threshold of less than 0.05 for entry. Apply Bonferroni to mitigate the problem with the p-values of the stepwise regression. This should help to avoid p-hacking and ensure the results are reliable. Thus, a relationship model has been established. To ensure the environmental factors at the 'collection point', the environmental factors within a 1 km × 1 km area were used to predict the quality suitability area. Finally, the spatial distribution map of the component was generated using the raster calculator, and the amygdalin content distribution map was overlaid with the species' ecological suitability map using the fuzzy overlay function to derive both current and future suitability distribution maps for quality [42].

Results

ITS2 identification and content determination results

The 26 sample batches from various origins were identified as belonging to the same species and were grouped into a single cluster (Fig. 2). The results show that the phylogenetic tree can distinguish the genetic

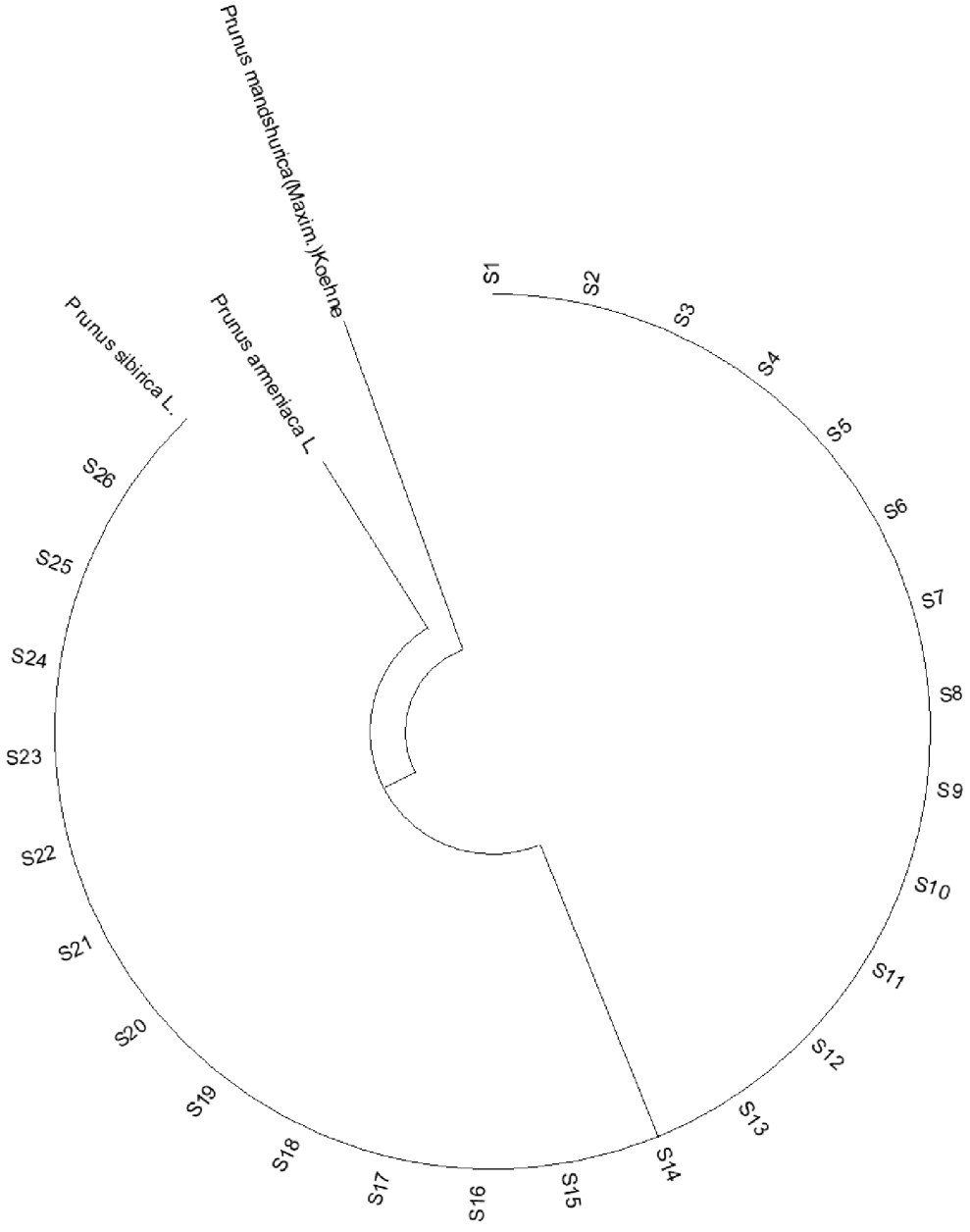

Fig. 2 Phylogenetic tree of 26 batches of samples

evolutionary relationships among the samples, providing a basis for determining the species origin of SAA. Subsequently, the amygdalin content in the 26 sample batches was quantified, with the results presented in Table 3.

Model evaluation

In this study, the AUC values for PM, PA, PS, and PK were 0.984, 0.954, 0.976, and 0.992, respectively (Fig. S1). The tAUC values are 0.986, 0.962, 0.980 and 0.993 respectively.

Variable importance

The values shown in the table (Table S1-S4) represented the average percentage contributions from 10 independent runs. The results showed that Bio 12 (45.1%) exerted the greatest influence on PM, followed by Bio 14 (19.7%) and Bio 6 (16.5%), contributing a cumulative total of 81.3%. Bio 12 (33.3%), Bio 6 (24.2%), and Bio 5 (16.1%) showed high permutation importance (PI) (Table S1). The jackknife plot (Fig. S2A) identified Bio 12, Bio 14, and Bio 6 as the three most important factors influencing PM distribution. The response curves for the primary environmental factors showed that Bio 6, Bio 5, Bio 12, and Bio 14 significantly influenced PM distribution (Fig. 3). The suitable range for Bio 6 spanned from −12.5 °C to -4.5 °C, with the optimal temperature near −9 °C. The suitable range for Bio 12 spanned from 500 mm to 800 mm, with the optimal precipitation near 530 mm. The suitable range for Bio 14 spanned from 2 mm to 10 mm, with the optimal precipitation near 4 mm. The suitable range for Bio 5 spanned from 25 °C to 32 °C, with the optimal temperature near 28 °C.

Table 3 Results of amygdalin content

Number	Latitude (*N*/°)	Longitude (E/°)	Amygdalin (%)
S1	39.90421	116.4074	3.4
S2	37.96857	109.3005	2.74
S3	37.95721	110.9984	3.14
S4	37.50891	110.2694	3.64
S5	48.01361	122.7375	1.83
S6	37.84968	110.1085	0.95
S7	41.57982	120.4575	2.87
S8	40.41279	118.9565	1.06
S9	37.07023	114.4923	3.76
S10	43.96809	119.3756	4.11
S11	41.22537	119.8096	3.05
S12	41.93435	117.7605	3.77
S13	36.69373	110.9407	1.14
S14	38.0037	110.5068	2.91
S15	37.75535	110.1839	0.55
S16	40.82467	119.8365	3.02
S17	37.08891	110.1214	1.11
S18	41.5331	121.2415	3.99
S19	122.995	41.1087	3.69
S20	115.832	40.9128	2.79
S21	106.4642	35.8571	4.11
S22	107.855	36.98991	4.41
S23	119.643	41.4031	3.24
S24	105.724	35.52346	2.71
S25	121.3489	42.03626	4.19
S26	118.0662	43.9529	2.74

Bio 17 (35.6%), Bio 5 (20.1%), and Bio 10 (13.7%) were the primary environmental factors influencing PA distribution, contributing a cumulative total of 69.4%. Based on permutation importance (PI), the three most influential environmental factors were Bio 1 (28.7%), Bio 5 (16.2%), and Bio 4 (10.1%) (Table S2). The jackknife plot of the Maxent model (Fig. S2B) identified Bio 1, Bio 12, and Bio 2 as the most important factors shaping PA habitat distribution. The response curves of the primary environmental factors (Fig. 4) revealed that precipitation in Bio 1, Bio 5, Bio 12, and Bio 17 all exhibited a distribution probability that first increased and then decreased with rising values, highlighting their impact on PA. Specifically, the optimal temperature range for Bio 1 spanned 7 °C to 16.5 °C, with the optimal temperature near 8 °C. The optimal precipitation range for Bio 17 spanned 10 mm to 45 mm, with the optimal precipitation near 17 mm. The suitable precipitation range for Bio 12 spanned 500 mm to 1100 mm, with the optimal precipitation near 650 mm. The optimal temperature range for Bio 5 spanned 26 °C to 32 °C, with the optimal temperature near 30 °C.

In PS, Bio 18 (36.9%), Bio 4 (36.1%), and Bio 15 (13.2%) had significant impacts, collectively contributing 86.2%. Bio 15 (35.5%), Bio 18 (19.4%), and Bio 10 (14.3%) demonstrated high permutation importance (PI) (Table S3). Analysis of the jackknife plot (Fig. S2C) indicated that Bio 10, Bio 18, and Bio 8 were the three most influential factors shaping the distribution of PS. The response curves of the primary ecological factors (Fig. 5) showed that Bio 15, Bio 10, Bio 8, and Bio 18 were key factors influencing the distribution of PS. Specifically, the suitable range for Bio 15 exceeded 110, while for Bio 18, it spanned from 240 mm to 400 mm, with the optimal precipitation around 265 mm. The suitable range for Bio 10 ranged from 19.5 °C to 23.5 °C, with the optimal temperature around 22 °C. The suitable range for Bio 8 ranged from 19.5 °C to 23.5 °C, with the optimal temperature around 22 °C.

In PK, Bio 4 (43.2%), Bio 12 (27.6%), and Bio 17 (17.8%) exerted significant impacts, contributing a total of 88.6%. Bio 1 (43.1%), Bio 10 (23.7%), and Bio 17 (11.8%) demonstrated high permutation importance (PI) (Table S4). The jackknife plot (Fig. S2D) showed that Bio 12, Bio 17, and Bio 4 were the three most influential factors shaping the distribution of PK. The response curves of the primary ecological factors (Fig. 6) revealed that Bio 4, Bio 10, Bio 12, and Bio 17 were key factors driving the distribution

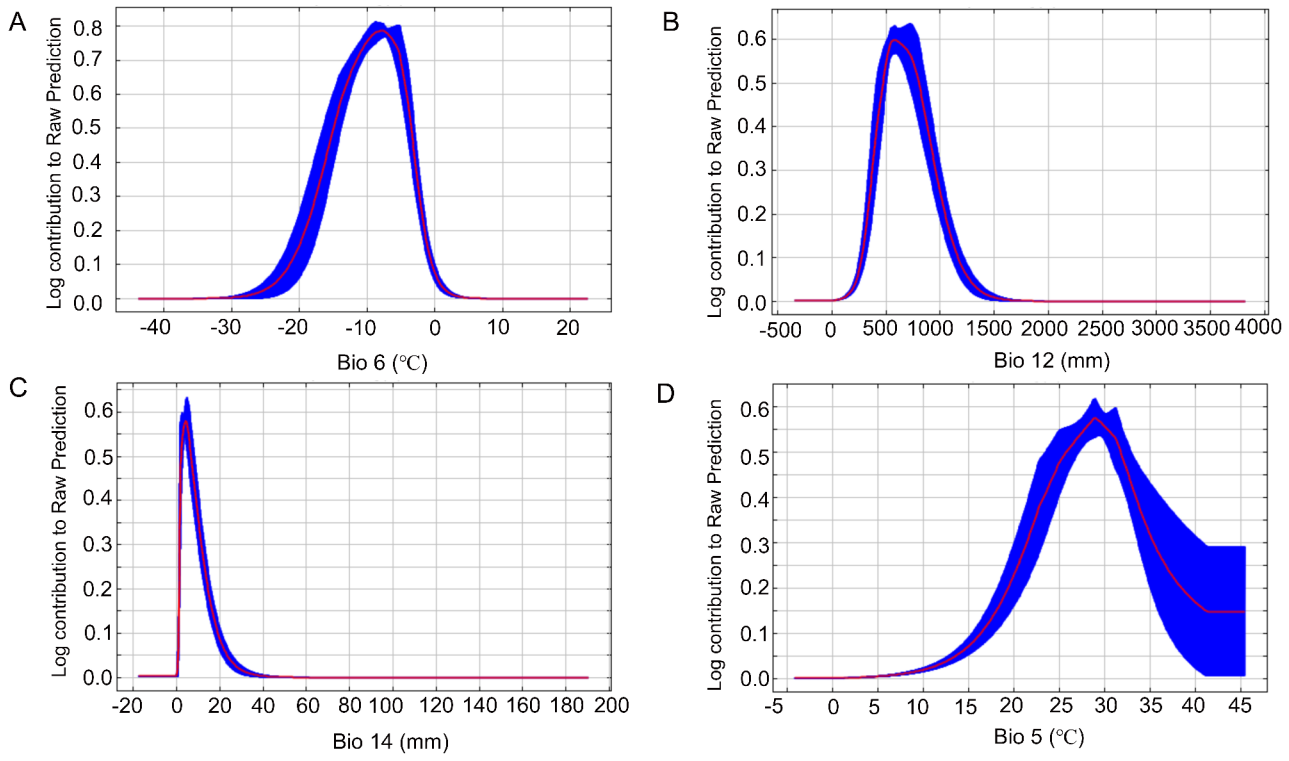

Fig. 3 Response curves of the effects of current climatic conditions on environmental variables related to symptom distribution in *Prunus armeniaca* L. var. ansu Maxim. (**A**-**D**). **A**: Bio6; **B**: Bio12; **C**: Bio14; **D**: Bio5

of PK. Specifically, the suitable range for Bio 4 spanned from approximately 12,500 to 14,000, with the optimal value near 13,500. The suitable range for Bio 10 spanned from 19 °C to 22.5 °C, with the optimal temperature around 21 °C. The suitable precipitation range for Bio 12 spanned from 520 mm to 980 mm, with the optimal precipitation around 735 mm. The suitable precipitation range for Bio 17 spanned from 20 mm to 38 mm, with the optimal precipitation around 28 mm.

Distribution prediction under modern conditions

The Maxent model predicted significant differences in the suitable distribution areas of the four plant species under current climatic conditions (Figs. 7A, 8A and 9A, and 10A). The suitable distribution area for PS is primarily located in northern and northeastern China, while PA and PM are predominantly at the junction of northwestern and northern China. PK is mainly distributed in the northeastern region. The main predicted distribution areas of PM, PA, PS, and PK are shown in the Table 4. The suitable area of PM reaches 1.19×10^6 km², accounting for 12.39% of the total area of China. The highly suitable areas are mainly distributed in Hebei Province, Tianjin, Henan Province, Shandong Province, Shaanxi Province, Shanxi Province, and Gansu Province, with an area of 0.209×10^6 km², accounting for 2.18% of the total area of China. The suitable area of PA reaches 2.7816×10^6 km², accounting for 28.98% of the total area of China. The highly suitable areas are mainly distributed in parts of western Xinjiang, Yunnan, eastern Tibet, eastern and southern Sichuan, Guizhou, Inner Mongolia Autonomous Region, Hebei Province, Tianjin, Henan Province, Liaoning Province, Shandong Province, Shaanxi Province, Shanxi Province, Gansu Province, Hubei Province, Hunan Province, and Qinghai Province, with an area of 0.446×10^6 km², accounting for 4.64% of the total area of China. The suitable area of PS is 1.69×10^6 km², accounting for 17.60% of the total area of China. The highly suitable areas are mainly distributed in central Hebei Province and southern Liaoning Province, with an area of 0.138×10^6 km², accounting for 1.44% of the total area of China. The suitable area of PK is 0.428×10^6 km², accounting for 4.45% of the total area of China. The highly suitable areas are mainly distributed in Jilin and Liaoning provinces, with an area of 0.109×10^6 km², accounting for 1.13% of the total area of China. (Table S5, Table S6, Table S7, and Table S8).

Distribution prediction under future conditions

Future projections suggests that the suitable habitat range for PM would both increase and decrease under different conditions. RCP2.6–2050 s、RCP2.6–2070 s and RCP8.5–2050 s are increase, RCP4.5–2050 s 、RCP4.5–2070 s and RCP8.5–2070 s are decrease (Fig. 7B-G). The

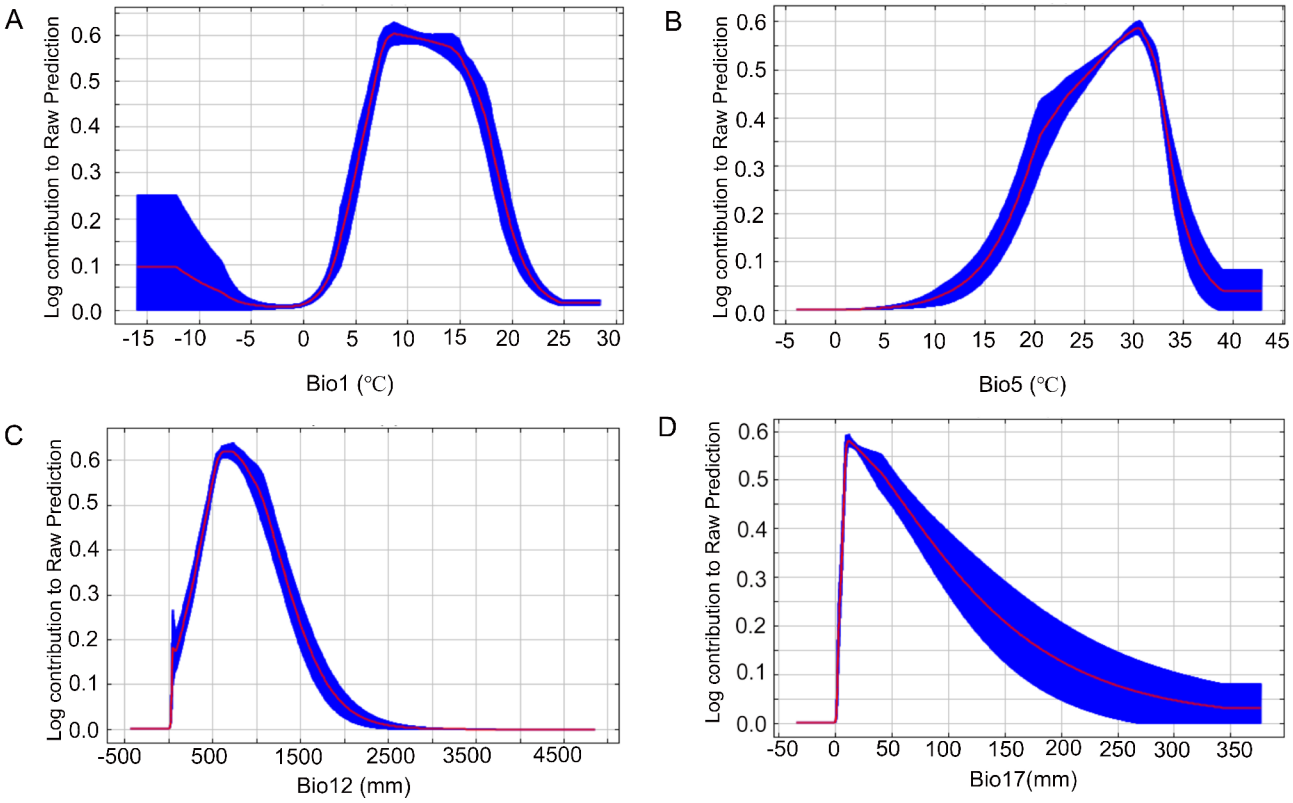

Fig. 4 Response curves of the effects of current climatic conditions on environmental variables related to symptom distribution in *Prunus armeniaca* L. (**A**-**D**). **A**: Bio1; **B**: Bio5; **C**: Bio12; **D**: Bio17

suitable habitat range for high-suitability areas of PA and PS generally decreases (Figs. 8B-G and 9B-G). However, the high-suitability areas for PS showed an increasing trend, while the suitable habitat range for PK generally expanded (Fig. 10B-G). Specifically, under the RCP2.6 emission scenario, the total suitable area for PA decreases by 11.96% in 2050 and 9.73% in 2070, compared to the present period. The total suitable area for PS decreased by 6.77% in 2050 and 16.43% in 2070. The total suitable area for PK increased by 7.24% in 2050 and 8.87% in 2070. The total suitable area for PM increased by 3.11% in 2050 and 3.45% in 2070. Under the RCP4.5 emission scenario, the total suitable area for PA decreased by 11.99% in 2050 and 6.59% in 2070. The total suitable area for PS decreased by 6.53% in 2050 and 7.89% in 2070. The total suitable area for PK increased by 8.64% in 2050 and 5.84% in 2070. The total suitable area for PM decreased by 2.18% in 2050 and 7.56% in 2070. Under the RCP8.5 emission scenario, the total suitable area for PA decreased by 11.99% in 2050 and 9.32% in 2070. The total suitable area for PS decreased by 9.54% in 2050 and increased by 0.7% in 2070. The total suitable area for PK increased by 5.84% in 2050 and 6.07% in 2070. The total suitable area for PM increased by 3.78% in 2050 and decreased by 1.01% in 2070. Moreover, the areas of medium and low suitability for PA declined substantially, whereas the high-suitability area remained relatively stable. Under different emission scenarios, the areas of medium and low suitability for PS decreased to varying extents, whereas the high-suitability area increased. Across different emission scenarios, the areas of high, medium, and low suitability for PK generally exhibited a sustainable expansion, with minor decreases in certain periods. PM showed a large range of changes, either increasing or decreasing.

Quality suitability analysis of PS

The analysis was conducted on the 14 samples from different origins with qualified amygdalin content. (Table 5). A relationship model between amygdalin content and environmental factors were developed using stepwise regression analysis. The regression model linking amygdalin content to environmental factors were expressed as $Y_1 = 12.435 - 0.095 \times X_1 - 0.097 \times X_2 + 0.086 \times X_3 + 0.047 \times X_4 + 0.073 \times X_5 - 0.017 \times X_6$ (The *p*-values after Bonferroni correction are all less than 0.01), where Y_1 represented the amygdalin content in PS, X_1 represented the Bio 6, X_2 represented the Bio 7, X_3 represented the Bio 8, X_4 represented the Bio 15, X_5 represented the Bio 17, and X_6 represented the Bio 18. According to the regression equation, amygdalin content was negatively correlated with the Bio 6, the Bio 7, and the Bio 18, while being

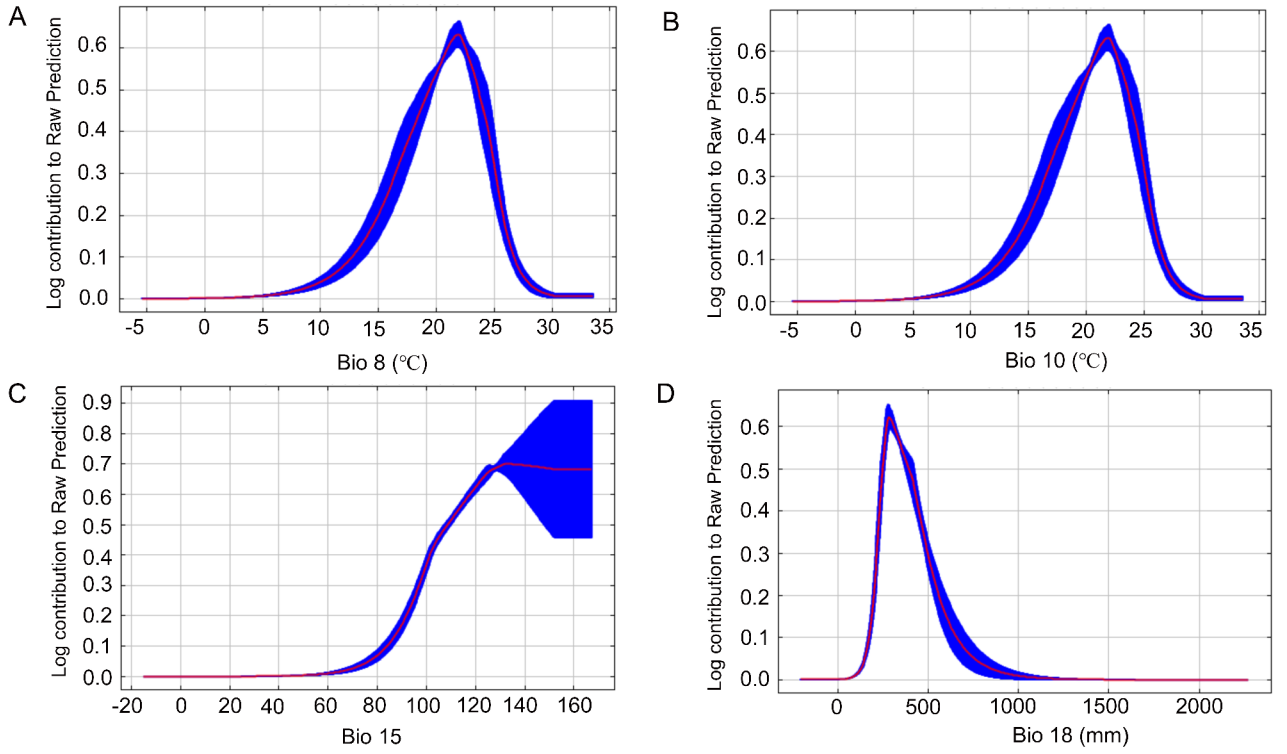

Fig. 5 Response curves of the effects of current climatic conditions on environmental variables related to symptom distribution in *Prunus sibirica* L. (**A**-**D**). **A**: Bio8; **B**: Bio10; **C**: Bio15; **D**: Bio18

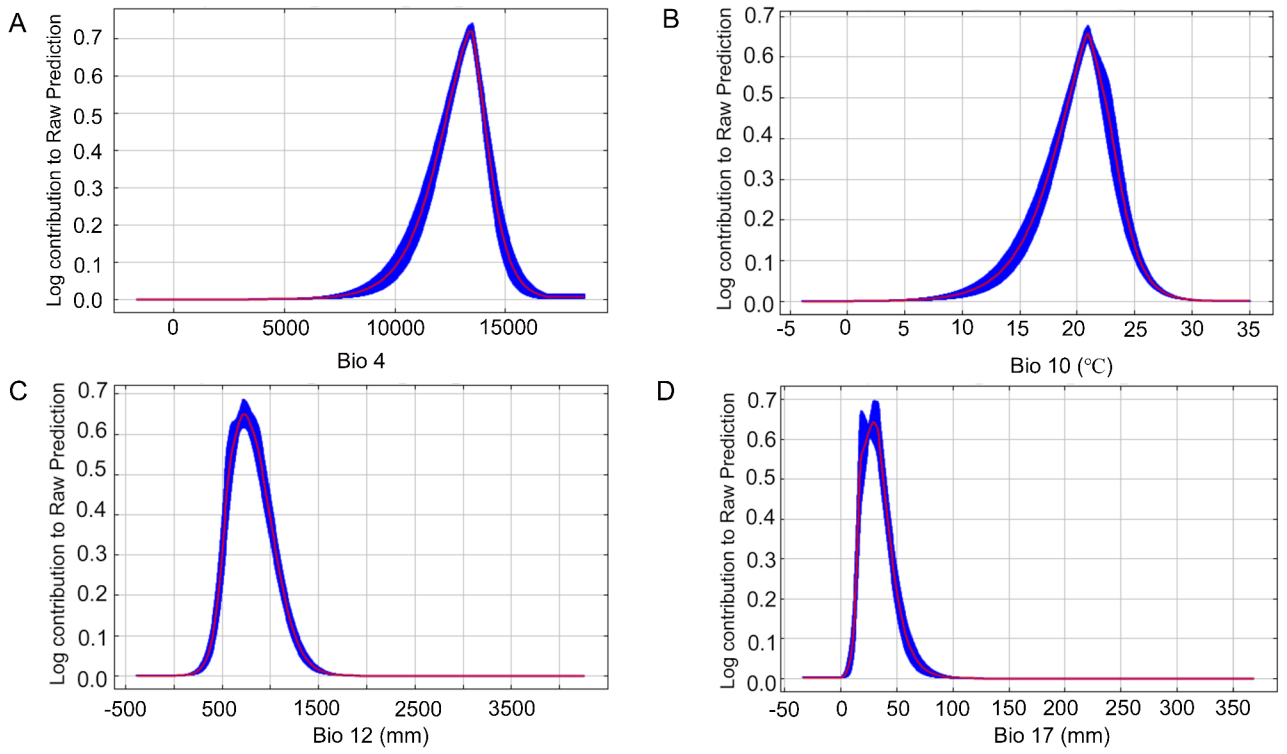

Fig. 6 Response curves of the effects of current climatic conditions on environmental variables related to symptom distribution in *Prunus mandshurica* (Maxim.) Koehne (**A**-**D**). **A**: Bio4; **B**: Bio10; **C**: Bio12; **D**: Bio17

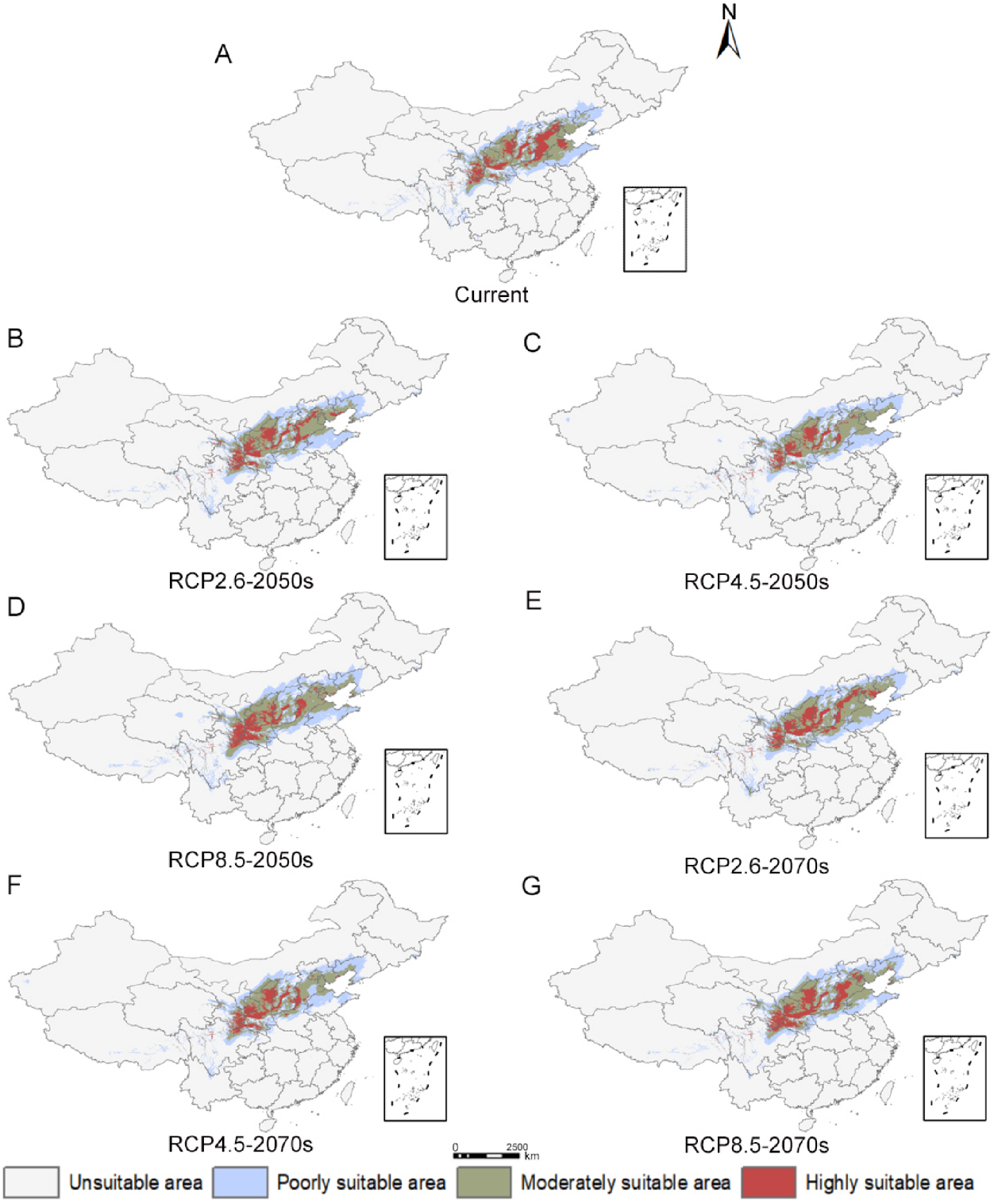

Fig. 7 The distribution of suitable areas of *Prunus armeniaca* L. var. ansu Maxim. under current climatic conditions (**A**) and the changes under three future climatic scenarios (**B**-**G**) (2050s, 2070s)

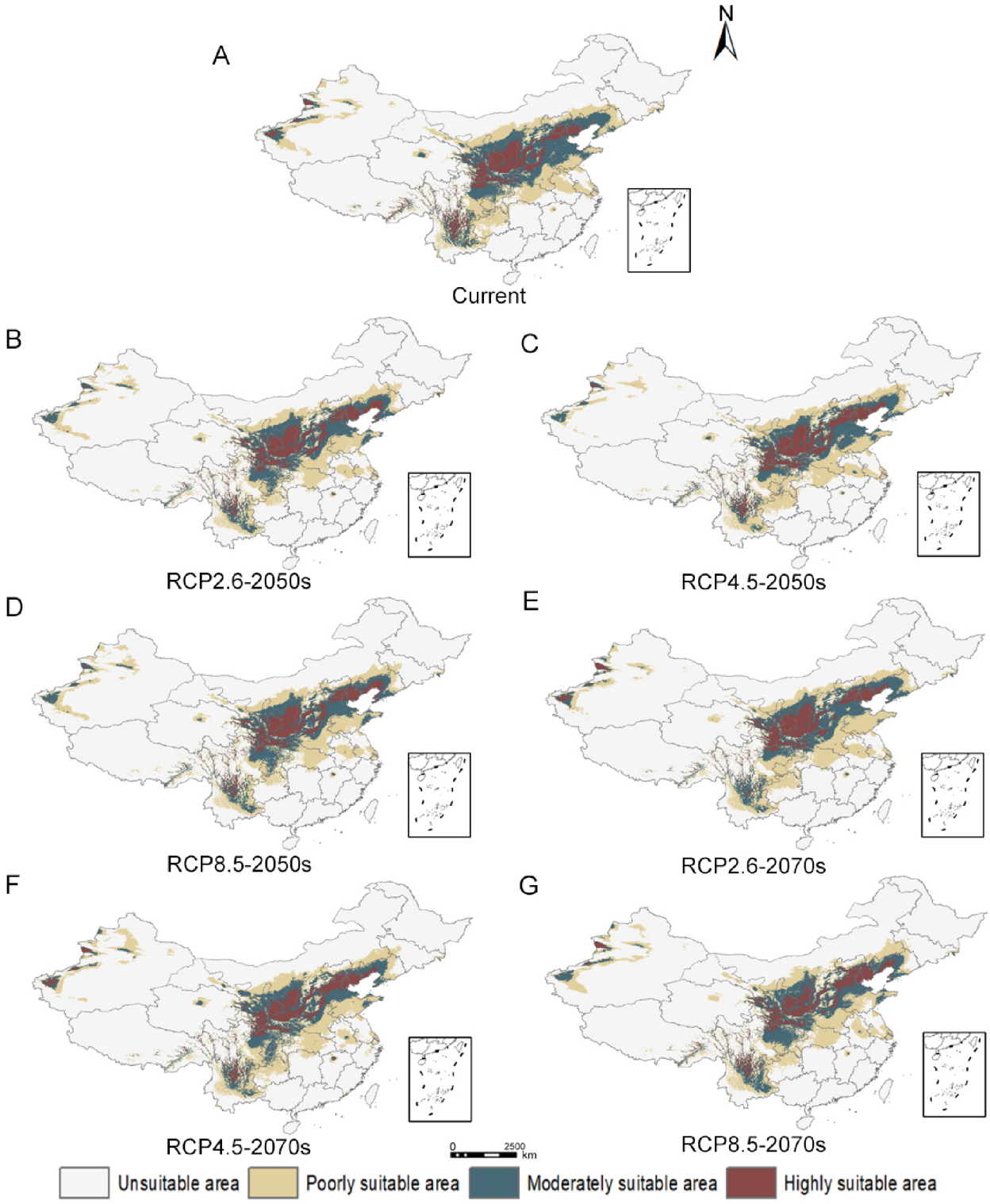

Fig. 8 The distribution of suitable areas of *Prunus armeniaca* L. under current climatic conditions (**A**) and the changes under three future climatic scenarios (**B**-**G**) (2050s, 2070s)

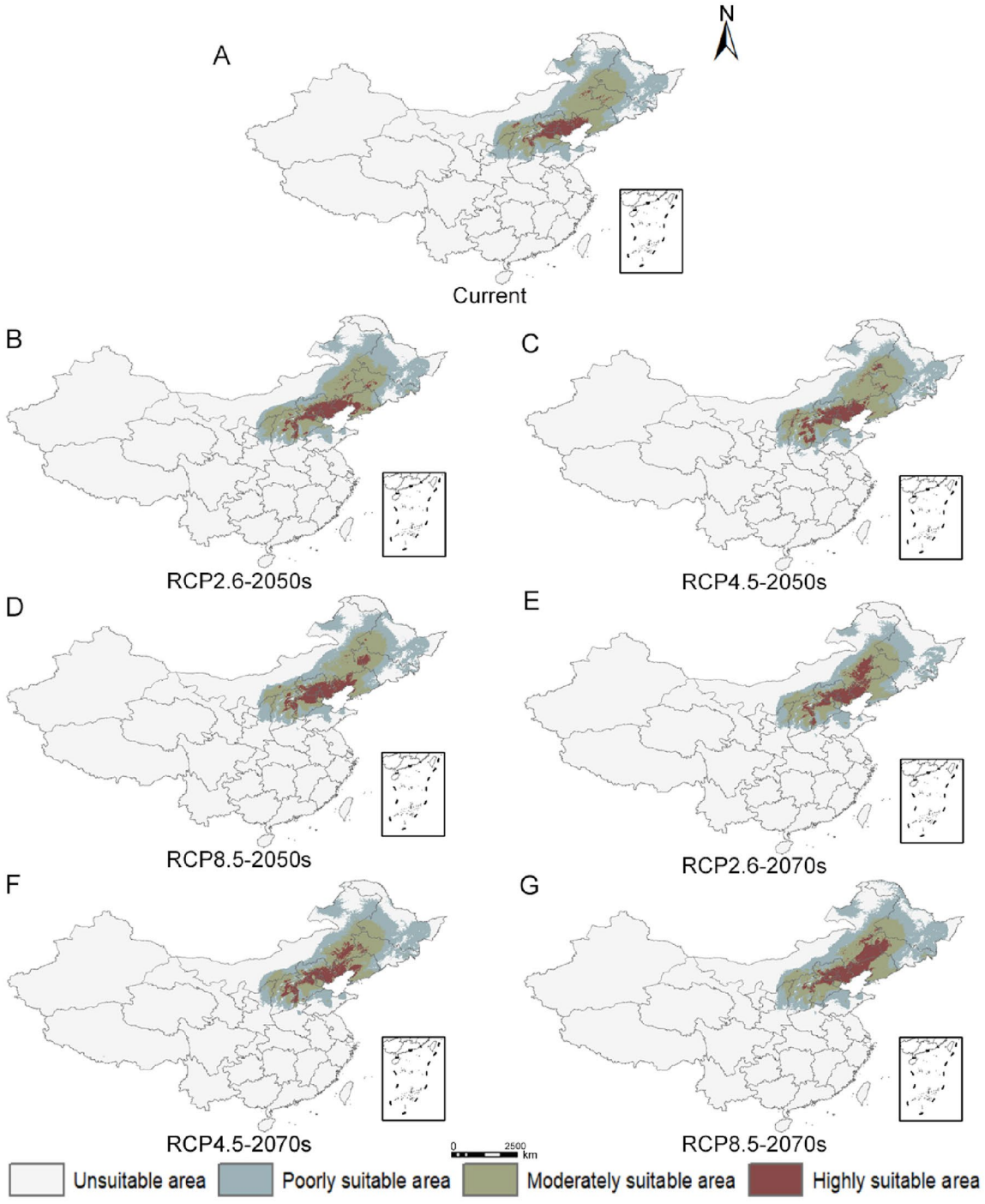

Fig. 9 The distribution of suitable areas of *Prunus sibirica* L. under current climatic conditions (**A**) and the changes under three future climatic scenarios (**B**-**G**) (2050s, 2070s)

positively correlated with the mean temperature of the Bio 8, the Bio 15, and the Bio 17 (Fig. S3).

Modern quality suitability of PS

The current quality zoning of PS is presented in Fig. 11A. The results indicated that amygdalin content was higher in regions with high suitability. The area suitable for amygdalin quality constituted 17.43% of the total area. The highest-quality areas were located in central Hebei Province, central Shanxi Province, western Liaoning Province, and parts of Inner Mongolia and Jilin, covering 6.22% of the total suitable area (0.104×10^6 km^2). The majority of Hebei Province, Heilongjiang Province, Jilin Province, Liaoning Province, Shanxi Province, Inner

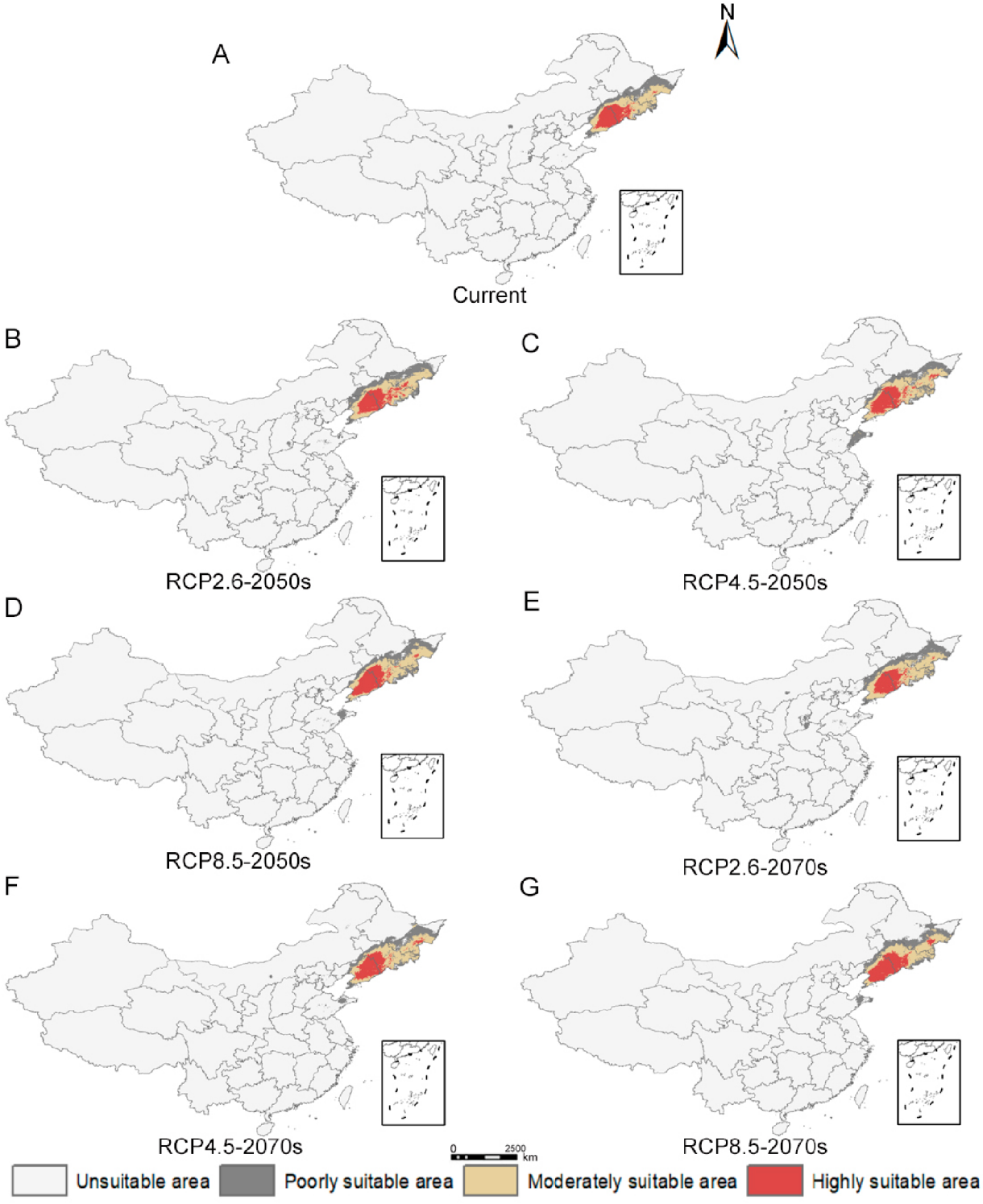

Fig. 10 The distribution of suitable areas of *Prunus mandshurica* (Maxim.) Koehne under current climatic conditions (**A**) and the changes under three future climatic scenarios (**B**-**G**) (2050s, 2070s)

Mongolia, and Shandong Province consisted of medium- and low-suitability areas for amygdalin quality, comprising 41.42% and 52.36% of the total suitable area, or 0.693×10^6 km² and 0.876×10^6 km² (Table 6).

Future quality suitability of PS

As depicted in the future predicted distribution maps (Fig. 11B-G), the changes in the suitable areas for amygdalin quality largely mirrored those in the

Table 4 The main predicted distribution areas

Species	Suitable area
PM	Beijing, Tianjin, Hebei Province, Henan Province, Shandong Province, Shanxi Province, Shaanxi Province, Ningxia Hui Autonomous Region, Gansu Province, Qinghai Province, Liaoning Province, and other places.
PA	Beijing, Hebei Province, Tianjin, Henan Province, Shandong Province, Shanxi Province, Shaanxi Province, Ningxia Hui Autonomous Region, Gansu Province, Inner Mongolia Autonomous Region, Qinghai Province, and Liaoning Province.
PS	northern Shaanxi Province, eastern Inner Mongolia Autonomous Region, Shanxi Province, Hebei Province, Beijing, Tianjin, northern Shandong Province, Heilongjiang Province, Jilin Province, and Liaoning Province
PK	Heilongjiang Province, Jilin Province, Liaoning Province, and small portions of Inner Mongolia Autonomous Region

Table 5 Fourteen sampling points that Meet the content determination standards

Number	Latitude(*N*/°)	Longitude(E/°)	Amygdalin(%)
1	39.90421	116.4074	3.40
2	37.95721	110.9984	3.14
3	37.50891	110.2694	3.64
4	37.07023	114.4923	3.76
5	43.96809	119.3756	4.11
6	41.22537	119.8096	3.05
7	41.93435	117.7605	3.77
8	40.82467	119.8365	3.02
9	41.5331	121.2415	3.99
10	122.995	41.1087	3.69
11	106.4642	35.8571	4.11
12	107.855	36.98991	4.41
13	119.643	41.4031	3.24
14	121.3489	42.03626	4.19

species distribution across all emission scenarios. With the exception of a slight increase under the RCP8.5–2070 s scenario, the total suitable area showed a progressive decrease across the emission scenarios. The high-suitability areas for amygdalin quality increased significantly under all scenarios. The medium-suitability areas exhibited a decreasing trend across all scenarios. The low-suitability areas demonstrated a slight increase under the RCP8.5–2070 s scenario, but decreased under the other scenarios.

Migration trend of the geometric center of the PS mass distribution

The most suitable habitat for the potential geometric center of amygdalin quality in modern PS illustrated in Fig. 12 was in Aohan Banner, Chifeng City, Inner Mongolia Autonomous Region (119.956569°E, 42.98438°N). Under the RCP2.6 scenario, PS shifted 62.97 km within Aohan Banner, followed by an additional 22.36 km of migration. Under the RCP4.5 scenario, PS migrated 113.62 km from Aohan Banner to Jianping County, Chaoyang City, Liaoning Province, followed by a return migration of 75.88 km to Aohan Banner. Under the RCP8.5 scenario, PS initially migrated 48.93 km within Aohan Banner, followed by an additional 24.67 km of migration. This indicated that, under future global warming scenarios, although the growth areas of PS might have experienced varying degrees of increase or decrease, the overall distribution changes remained minimal.

Discussion

PM, PS, PK, and PA are important fruit tree species native to China, widely utilized in traditional Chinese medicine and recognized for their diverse ecological roles. However, these species are increasingly threatened by climate change [43], and the sustainable utilization of SAA is constrained by unsystematic resource exploitation and quality variability among its botanical sources. Amygdalin, the principal marker compound of SAA, is widely regarded as a key indicator of its medicinal quality [8].

Amygdalin is a cyanogenic glycoside belonging to the glucoside family and is widely recognized as a representative plant secondary metabolite. According to the optimal defense hypothesis, secondary metabolites serve primarily defensive roles, particularly in species with limited regenerative capacity, with their protective benefits increasing under environmental stress. Consequently, plants often upregulate secondary metabolite production in response to abiotic stress conditions [44]. Cyanogenic glycosides are hydrolyzed by β-glucosidase to yield α-hydroxy nitrile and glucose. The α-hydroxy nitrile is then enzymatically converted into hydrogen cyanide, a highly toxic compound, by α-hydroxy nitrile lyase, which acts as a chemical defense against herbivores and pathogens [45]. Notably, low temperatures can significantly alter the abundance and composition of plant secondary metabolites. For instance, low temperatures have been shown to elevate quercetin mannoside levels in *Brassica oleracea* var. *sabellica* [46] and to enhance alkyl glucoside accumulation in *Brassica oleracea* L. var. *italica* Plenck [47]. Drought stress has also been reported to exert a more pronounced influence on the biosynthesis of secondary metabolites. Cyanogenic glycoside concentrations often increase in response to drought conditions. For example, *Phaseolus lunatus* L. showed increased cyanogenic glycoside concentrations under drought stress, possibly reflecting a defensive adaptation to water-deficit environments [48]. Our findings revealed a significant negative correlation between amygdalin content and key environmental variables, including the

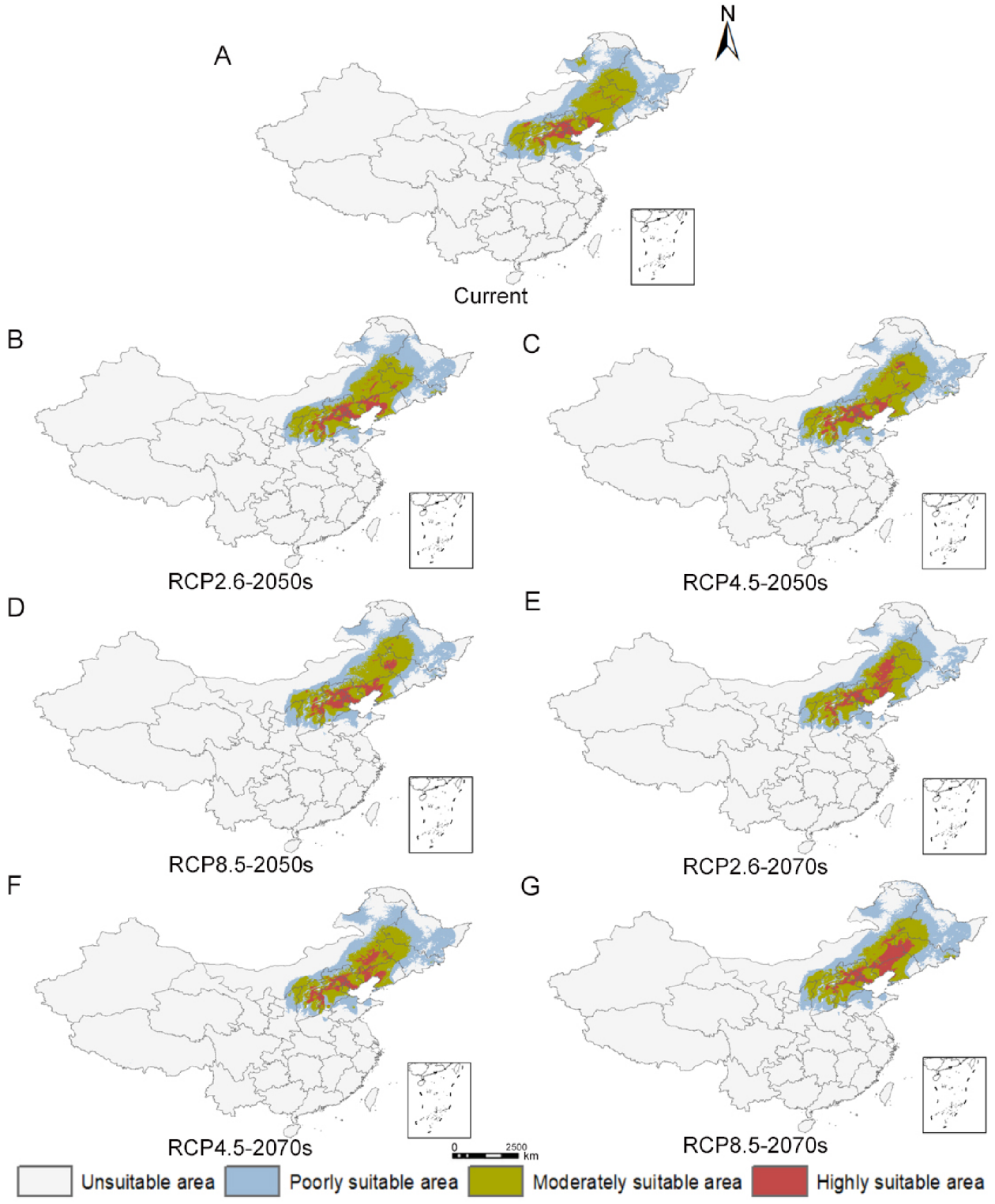

Fig. 11 The quality regionalization of amygdalin under current climatic conditions (**A**) and the changes in the quality regionalization of amygdalin under three future climatic scenarios (**B**-**G**) (2050s, 2070s)

Table 6 Quality suitable area of amygdalin based on current and future climate conditions

Different periods of amygdalin	Highly suitable area/×10^6 km^2	Moderately suitable area/×10^6 km^2	Poorly suitable area/×10^6 km^2	Suitable area/×10^6 km^2
Current	0.104	0.693	0.876	1.673
RCP2.6–2050 s	0.141	0.643	0.773	1.557
RCP2.6–2070 s	0.160	0.565	0.673	1.398
RCP4.5–2050 s	0.139	0.669	0.748	1.556
RCP4.5–2070 s	0.161	0.569	0.811	1.541
RCP8.5–2050 s	0.157	0.604	0.756	1.517
RCP8.5–2070 s	0.207	0.596	0.880	1.683

minimum temperature of the coldest month, variability in mean annual temperature, and precipitation during the warmest quarter. This trend is consistent with previously reported increases in amygdalin accumulation under low-temperature and drought stress conditions. A Maxent-based study on the potential geographic distribution and habitat suitability of *Rosa banksiae* Aiton in China identified the minimum temperature of the coldest month as the most influential variable, followed by annual precipitation [49]. These findings underscore the central role of temperature and precipitation in determining the ecological distribution of *Rosa* species.

In recent years, research on SAA has largely concentrated on product processing and related areas; however, substantial discrepancies across studies have reduced their applicability to large-scale cultivation and production. Variations in varietal quality and suitable cultivation zones further constrain the comprehensive utilization of SAA resources. Our study projected the climatic range of four SAA producing tree species and the amygdalin quality zoning of one of those species. By doing so we aimed to investigate the primary climatic factors affecting the distribution of those SAA producing species and identify their optimal climatic areas. Our results indicated that PS is primarily suited to northern and northeastern China; PA and PM are concentrated at the junction of northwest and northern China; and PK is mostly distributed in the northeast. Although distribution ranges shifted under future climate scenarios, none of the four

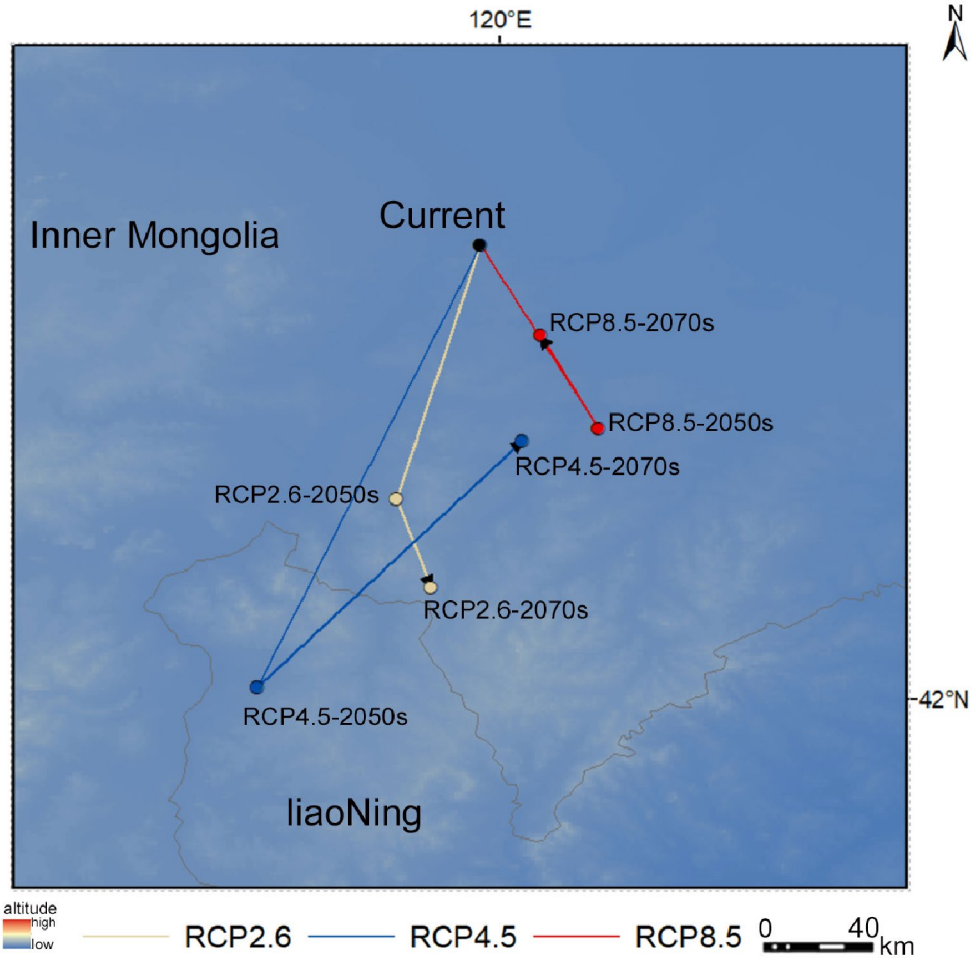

Fig. 12 The centroid migration diagram of the *Prunus sibirica* L. quality of the suitable habit

species exhibited statistically significant changes. Taking PS as a case study, we examined the correlation between amygdalin content and environmental variables. Further analysis revealed that lower temperatures and decreased precipitation were associated with increased amygdalin accumulation. Appropriate agronomic interventions in moderately or marginally suitable zones may enhance amygdalin content, offering practical guidance for improving cultivation outcomes. However, the accuracy of the Maxent model strongly depends on the quality of species distribution data. Insufficient sampling or poorly resolved environmental variables may lead to inaccurate model predictions. These limitations were evident in PK, which had relatively few recorded distribution sites. Moreover, our model focused exclusively on climatic variables, omitting key factors such as species interactions, anthropogenic disturbances, soil characteristics, topography, and biotic constraints (e.g., pests or pollinator availability), which may have resulted in overestimated distribution ranges [50]. A related study utilizing a global tree database found that human activities were the strongest predictors of non-native species establishment, while greater native tree diversity reduced invasion severity. Although temperature and precipitation influenced invasion strategies, their effects were attenuated in regions with intensive human activity [51]. These findings provide valuable insights for managing local species invasions. Given the high market demand for SAA in traditional Chinese medicine, protected areas can be established based on predicted suitability zones and actual growing regions. Species-specific planting strategies can be formulated according to the predicted distribution patterns. Additionally, environmental interventions-such as weather warning systems, pest control measures, and irrigation infrastructure may help optimize growing conditions and improve plant performance [52–53].

Conclusions

Our study predicted the potential distributional shifts of four SAA source tree species and modeled the spatial distribution of amygdalin content using PS as a representative. Based on these findings, targeted environmental interventions can be implemented to optimize growing conditions, and conservation zones can be designated for species best adapted to specific regions. In areas where certain species are poorly adapted, large-scale harvesting can be followed by the introduction of more ecologically appropriate alternatives. Furthermore, spatial variation in amygdalin content, when aligned with pharmacopoeial standards, can inform precision harvesting strategies to ensure consistent medicinal quality. Collectively, these strategies provide actionable insights for the conservation and long-term sustainable use of SAA resources.

Supplementary Information

The online version contains supplementary material available at https://doi.org/10.1186/s12870-025-06627-2.

Supplementary Material 1

Acknowledgements
Not applicable.

Author contributions
ZL and DM contributed to the research design. ZX and ZY contributed to the experiments. LC and XD contributed data analysis. XG, YY, and KZ contributed to manuscript writing and revising. All authors contributed to the article and approved the submitted version.

Funding
This research was supported financially by the Innovation Team of Hebei Province Modern Agricultural Industry Technology System (No. HBCT2024110201), the Scientific and Technological Project of Shijiazhuang City of Hebei Province (No. 241200013 A), and the Scientific research project of Hebei Administration of Traditional Chinese Medicine (No. 2025069).

Data availability
The authors confirm that the data supporting the findings of this study are available within the article [and/or] its supplementary materials.Sequence data that support the findings of this study have been deposited in the Genbank repository with the primary accession code PV174600-PV174625 (persistent web link: https://submit.ncbi.nlm.nih.gov/subs/?search=SUB15112251).

Declarations

Ethics approval and consent to participate
Not applicable.

Consent for publication
Not applicable.

Competing interests
The authors declare no competing interests.

Author details
[1]Hebei University of Traditional Chinese Medicine, Shijiazhuang, Hebei 050200, China
[2]International Joint Research Center on Resource Utilization and Quality Evaluation of Traditional Chinese Medicine of Hebei Province, Shijiazhuang, Hebei 050091, China
[3]Chengde Yaou Nuts & Seeds Co.,Ltd, Chengde 067500, China

Received: 18 February 2025 / Accepted: 25 April 2025
Published online: 07 May 2025

References

1. O'Connor B, Bojinski S, Röösli C, Schaepman ME. Monitoring global changes in biodiversity and climate essential as ecological crisis intensifies. Ecol Inf. 2020;55:101013.
2. Tan Z, Yuan YH, Huang SY, Ma YX, Hong ZY, Wang Y, et al. Geographical distribution and predict potential distribution of *Angelica* L.genus. Environ. Sci Pollut Res. 2023;30:46562–73.
3. Vermeulen SJ, Campbell BM, Ingram JSI. Climate change and food systems. Annu Rev Environ Resour. 2012;37:195–222.
4. Wiebe K, Robinson S, Cattaneo A. Climate change, agriculture and food security: impacts and the potential for adaptation and mitigation. Sustainable-food Agric, pp. 2019; 55–74.
5. Beridze B, Sękiewicz K, Walas Ł, Thomas PA, Danelia I, Fazaliyev V, et al. Biodiversity protection against anthropogenic climate change: conservation prioritization of Castanea sativa in the South Caucasusbased on genetic and ecological metrics. Ecol Evol. 2023;13(5):e10068.

6. Zhang QA, Yao JL. State-of-the-Art on the processing and comprehensive utilization of the apricot kernels. Scientia Agricultura Sinica. 2019;52(19):3430–47.
7. Zeng T, Sun X, Miao Y, Gu SJ, Tian LX, Zheng Y, et al. Integrating bioclimatic factors and secondary metabolism to predict the suitable producing area of plants with high specific metabolite content in a real-world environment-a case of *Carthamus tinctorius* L. Ind Crops Prod. 2022;177:114545.
8. Commission CP. Pharmacopoeia of the People's Republic of China. Volume I. Beijing: China Medical Science; 2020. p. 210.
9. Bai H, He MY, Xu Y, Jiang ZH, Gao P, Cong ZF. Research progress of traditional Chinese medicine Kuxingren (Armeniacae semen Amarum) and prediction of Lts Q-Markers. Chin Archives Traditional Chin Med. 2024;42(09):199–209.
10. Barakat H, Aljutaily T, Almujaydil MS, Algheshairy RM, Alhomaid RM, Almutairi AS, et al. Amygdalin: a review on its characteristics, atioxidant potential, Gastrointestinal microbiota intervention, anticancer therapeutic and mechanisms, toxicity, and encapsulation. Biomolecules. 2022;12(10):1514.
11. Mosayyebi B, Mohammadi L, Kalantary-Charvadeh A, Rahmati M. Amygdalin decreases adhesion and migration of MDA-MB-231 and MCF-7 breast cancer cell lines. Curr Mol Pharmacol. 2021;14(4):667–75.
12. Makarević J, Tsaur I, Juengel E, Borgmann H, Nelson K, Thomas C, et al. Amygdalin delays cell cycle progression and blocks growth of prostate cancer cells in vitro. Life Sci. 2016;147:137–42.
13. Abdel-Gawad DRI, Ibrahim MA, El-Banna HA, Hassan WH, Abo El-Ela FI. Evaluating the therapeutic potential of amygdalin: cytotoxic and antimicrobial properties. Tissue Cell. 2024;89:102443.
14. Applequist WL, Brinckmann JA, Cunningham AB, Hart RE, Heinrich M, Katerere DR, et al. Scientists' warning on climate change andmedicinal plants. Planta Med. 2020;86(1):10–8.
15. Cohen SD. Estimating the climate niche of *Sclerotinia sclerotiorum* using maximum entropy modeling. J Fungi (Basel). 2023;9(9):892.
16. Ganglo JC. Ecological niche model transferability of the white star Apple (*Chrysophyllum albidum* G. Don) in the context of climate and global changes. Sci Rep. 2023;13(1):2430.
17. Ngarega BK, Chaibva P, Masocha VF, Saina JK, Khine PK, Schneider H. Application of maxent modeling to evaluate the climate change effects on the geographic distribution of *Lippia Javanica* (Burm.f.) spreng in Africa. Environ Monit Assess. 2023;196(1):62.
18. Kumar D, Rawat S. Modeling the effect of climate change on the distribution of threatened medicinal Orchid *Satyrium Nepalense* D. Don in India. Environ Sci Pollut Res Int. 2022;29(48):72431–44.
19. Wouyou HG, Lokonon BE, Idohou R, Zossou-Akete AG, Assogbadjo AE, Glèlè Kakaï R. Predicting the potential impacts of climate change on the endangered *Caesalpinia bonduc* (L.) Roxb in Benin (West Africa). Heliyon. 2022;8(3):e09022.
20. Naudiyal N, Wang J, Ning W, Gaire NP, Peili S, Yanqiang W, et al. Potential distribution of abies, Picea, and Juniperus species in the subalpine forest of Minjiang headwater region under current and future climate scenarios and its implications on ecosystem services supply. Ecol Ind. 2021;121:107131.
21. Duan RY, Kong XQ, Huang MY, Fan WY, Wang ZG. The predictive performance and stability of six species distribution models. PLoS ONE. 2014;9(11):e112764.
22. Zhao ZY, Xiao NW, Shen M, Li JS. Comparison between optimized maxent and random forest modeling in predicting potential distribution: A case study with *Quasipaa boulengeri* in China. Sci Total Environ. 2022;842:156867.
23. Schnase JL, Carroll ML, Gill RL, Tamkin GS, Li J, Strong SL, et al. Toward a Monte Carlo approach to selecting climate variables in maxent. PLoS ONE. 2021;16(3):e0237208.
24. Boria RA, Olson LE, Goodman SM, Anderson RP. Spatial filtering to reduce sampling bias can improve the performance of ecological niche models. Ecol Modell. 2014;275:73–7.
25. Fourcade Y, Engler JO, Rödder D, Secondi J. Mapping species distributions with maxent using a geographically biased sample of presence data: a performance assessment of methods for correcting sampling bias. PLoS ONE 2014; 9(5), e97122.
26. Zhong JP, Yin HL, Zhang T, et al. Quality evaluation of Asparagus *cochinchinensis* based on ITS2 sequence and characteristic chromatogram. Chin Traditional Herb Drugs. 2024;55(22):7812–9.
27. Van Vuuren DP, Edmonds J, Kainuma M, Riahi K, Thomson A, Hibbard K, et al. The representative concentration pathways: an overview. Clim Change. 2011;109:5.
28. Abdelaal M, Fois M, Fenu G, Bacchetta G. Using maxent modeling to predict the potential distribution of the endemic plant Rosa Arabica Crép. In Egypt. Ecol Inf. 2019;50:68–75.
29. Jayasinghe SL, Kumar L. Modeling the climate suitability of tea [*Camellia sinensis* (L.) O. Kuntze] in Sri Lanka in response to current and future climate change scenarios. Agric Meteorol. 2019;272:102–17.
30. Li X, Gu X, Mao F, Guo H, Qiu J, Liu Y, Bi J, Wei T, Zheng Y, Zhao Y. Assessment of the potential habitat suitability and ephedrine quality of two Ephedra species in China under climate change. Plant Biosystems-An Int J Dealing all Aspects Plant Biology. 2024;158(3):479–89.
31. Li CW, Li DR, Wang RL et al. Studies on the effect of high temperature on the quality of bitter almonds. J Zhengzhou Inst Technol.2003; (04): 25–7.
32. Qiu HZ, Chen CY. Habitat suitability evaluation of ancient ginkgo trees in Changsha based on random forest and maxent model. Journalof Cent South Univ Forestry Technol. 2024;44(11):87–97.
33. Zhang H, Zhao HX, Wang H. Potential geographical distribution of populus euphratica in China under future climate change scenarios based on maxent model. Acta Ecol Sin. 2020;40(18):6552–63.
34. Pearson RG, Raxworthy CJ, Nakamura M, Peterson AT. Predicting species distributions from small numbers of occurrence records: a test case using cryptic geckos in Madagascar. J Biogeogr. 2007;34(1):102–17.
35. Halvorsen R. A maximum likelihood explanation of maxent, and some implications for distribution modelling. Sommerfeltia. 2013;36:1–132.
36. Wakie TT, Evangelista PH, Jarnevich CS, Laituri M. Mapping current and potential distribution of non-native *Prosopis juliflora* in the Afar region of Ethiopia. PLoS ONE 2014; 9(11), e112854.
37. Li JJ, Wu J, Peng KZ, Fan G, Yu HQ, Wang WG et al. Simulating the effects of climate change across the geographical distribution of two medicinal plants in the genus nardostachys. PeerJ. 2019; 7, e6730.
38. Sharma MK, Ram B, Chawla A. Ensemble modelling under multiple climate change scenarios predicts reduction in highly suitable range of habitats of Dactylorhiza Hatagirea (D. Don) Soo in Himachal Pradesh, Western Himalaya[J]. South Afr J Bot. 2023;154:203–18.
39. Shu YX, Sun KF, Xu WF, Chen YR, Sun QW, Wang B. Ecology suitability and quality regionalization analysis on Miao medicine Laportea bulbifera. Chin J Exp Form. 2023;29(03):160–9.
40. Commission CP. Pharmacopoeia of the People's Republic of China.Vol. I. Beijing: China Medical Science; p.; 2020. pp. 333–4.
41. Li J, Yu Y, Guo LP, Huang LQ, Zhang XB, Yang J. Study on quality regionalization of lycii fructus. China J Chin Mater Med. 2019;44(06):1156–63.
42. Shu YX, Sun KF, Xu WF, Chen YR, Sun QQ, Wang B. Ecology suitability and quality regionalization analysis on Miao medicine Laportea bulbifera. Chin J Exp Form. 2023;29(03):160–9.
43. Li M, Zhao Z, Miao XJ, Zhou JJ. Genetic diversity and population structure of Siberian apricot (Prunus sibirica L.) in China. Int J Mol Sci. 2013;15(1):377–400.
44. Su WH, Zhang GF, Li XH, Ou XK. Relationship between accumulation of secondary metabolism in medicinal plant and environmental condition. Chin Traditional Herb Drugs.2005; (09):139–42.
45. Duan S, Wu XT, Li B. Research progress in structure of amygdalin and its degradation process. Food Sci Technol. 2020;45(09):233237.
46. Neugart S, Kläring H-P, Zietz M, Schreiner M, Rohn S, Kroh LW, et al. The effect of temperature and radiation on flavonol aglycones and flavonol glycosides of Kale (Brassica Oleracea Var. sabellica). Food Chem. 2012;133:1456–65.
47. Schonhof I, Kläring H-P, Krumbein A, Clauβen W, Schreiner M. Effect of temperature increase under low radiation conditions on phytochemicals and ascorbic acid in greenhouse grown broccoli. Agric Ecosyst Environ. 2007;119:103–11.
48. Ballhorn DJ, Reisdorff C, Pfanz H. Quantitative effects of enhanced CO2 on jasmonic acid induced plant volatiles of lima bean (Phaseolus lunatus L). J Appl Bot Food Qual. 2011;84:65–71.
49. Wang LH, Qin H, Sun XF, Wang XY. Prediction of potential geographical distribution and habitat analysis of Rosa banksiae in China based on maxent model and ArcGIS. Chin Landsc Archit. 2023;39(06):120–6.
50. Wang LR, Li Q, Feng CH, Shi ZP. Predicting potential ecological distribution of locusta migratoria tibetensis in China using maxent ecological niche modeling. Acta Ecol Sin. 2017;37(24):8556–66.
51. Delavaux CS, Crowther TW, Zohner CM, et al. Native diversity buffers against severity of non-native tree invasions. Nature. 2023;621:773–81.
52. Skevas T, Massey R, Grashuis J. Farmer adoption and intensity of use of extreme weather adaptation and mitigation strategies: evidence from a sample of Missouri farmers. Clim Change. 2022;174:18.

53. Tanti PC, Jena PR, Timilsina RR, et al. Enhancing crop yields and farm income through climate-smart agricultural practices in Eastern India. Mitig Adapt Strateg Glob Change. 2024;29:35.

Publisher's note